AGU100 ADVANCING EARTH AND SPACE SCIENCE

Geophysical Research Letters

RESEARCH LETTER
10.1029/2019GL084675

Key Points:
- Abrupt BA warming was simulated under a gradual increase of insolation, greenhouse gases, and meltwater flux
- The timing of abrupt warming depended on the level of meltwater flux
- Gradual warming may have caused abrupt warming during the middle stage of the last deglaciation

Supporting Information:
- Supporting Information S1

Correspondence to:
T. Obase,
obase@aori.u-tokyo.ac.jp

Citation:
Obase, T., & Abe-Ouchi, A. (2019). Abrupt Bølling-Allerød warming simulated under gradual forcing of the last deglaciation. *Geophysical Research Letters*, *46*. https://doi.org/10.1029/2019GL084675

Received 23 JUL 2019
Accepted 24 SEP 2019
Accepted article online 10 OCT 2019

Abrupt Bølling-Allerød Warming Simulated under Gradual Forcing of the Last Deglaciation

Takashi Obase[1] and **Ayako Abe-Ouchi**[1,2,3]

[1]Atmosphere and Ocean Research Institute, The University of Tokyo, Kashiwa, Japan, [2]Japan Agency for Marine-Earth Science and Technology, Yokohama, Japan, [3]National Institute of Polar Research, Tachikawa, Japan

Abstract During the last deglaciation, a major global warming trend was punctuated by abrupt climate changes, likely related to Atlantic meridional overturning circulation (AMOC). One problem is that an abrupt increase in the AMOC during the Bølling-Allerød (BA) transition occurred when the melting of Northern Hemisphere ice sheets was significant, which tended to weaken the AMOC. Here, from transient simulations of the last deglaciation using an atmosphere-ocean general circulation model, we show that an abrupt increase in the AMOC during the BA transition could occur without reduction in glacial meltwater. The abrupt increase in the AMOC accompanied abrupt warming in Greenland and sea ice retreat in the North Atlantic, consistent with proxies and previous modeling studies. The results imply that abrupt BA warming during the middle stage of the last deglaciation was a response to gradual warming under the presence of meltwater from continental ice sheets.

1. Introduction

The transition from the Last Glacial Maximum (LGM) to the present interglacial occurred approximately 21,000 to 9,000 years ago, known as the last deglaciation and the last ice age termination (Clark et al., 2012; Denton et al., 2010). The melting of continental ice sheets raised the global mean sea level during the last deglaciation (Abe-Ouchi et al., 2013; Carlson & Clark, 2012). One remarkable point is that abrupt and large climate changes occurred during the middle stage of the last deglaciation, superimposed on gradual global warming (Clark et al., 2012; Shakun & Carlson, 2010). One event was the Bølling-Allerød (BA) transition (about 14.7 to 14.2 ka, Ivanovic et al., 2016), characterized by abrupt and drastic warming in Greenland (10 °C within a few decades, Buizert et al., 2014). During the BA interval (about 14.7 to 13 ka), the warming trend in Antarctica and the Southern Hemisphere stopped and turned into a cooling trend (Pedro et al., 2016). Reconstructions indicate that there was significant warming in the Southern Hemisphere during Heinrich 1 (H1, ~18 to 14.7 ka) just before BA (Shakun et al., 2012). Reconstructions also indicate that the Atlantic meridional overturning circulation (AMOC) was weaker and that North Atlantic Deep Water formation was shallower during H1 and rapidly increased in the BA transition (McManus et al., 2004; Roberts et al., 2010). The AMOC is commonly invoked to explain abrupt climate changes through the "bipolar seesaw" mechanism associated with the meridional heat transport of the AMOC (Broecker, 1998; Clark et al., 2002; Rahmstorf, 2002).

Transient simulation is suitable to understand the causes and mechanisms of the abrupt climate changes and the phase relationships of the last deglaciation. Recent studies have used atmosphere-ocean coupled general circulation models (AOGCMs) and conducted transient simulations of the last deglaciation. In these simulations, abrupt increase in the AMOC was simulated in response to cessation of meltwater input into the North Atlantic (He et al., 2013; Liu et al., 2009; Menviel et al., 2011). In contrast, gradual warming of the last deglaciation has been shown to have caused abrupt increase in the AMOC as the warming increased salinity transport from the South Atlantic, based on an ocean general circulation model (Knorr & Lohmann, 2003). In previous studies, abrupt increase in the AMOC has been explained by gradual meltwater input into the Southern Ocean reducing the density of bottom water mass originating from the Southern Ocean (Weaver et al., 2003), and the response to gradual orbital forcing under the presence of meltwater in the North Atlantic (Ganopolski & Roche, 2009), based on an Earth system model. Recently, AOGCM experiments showed that abrupt climate changes can be induced by gradual change in CO_2 concentration under the presence of meltwater and intermediate ice sheet (Zhang et al., 2017). It was shown that the state of the AMOC depends on the background climate (Brown & Galbraith, 2016; Kawamura et al., 2017; Klockmann et al.,

10.1029/2019GL084675

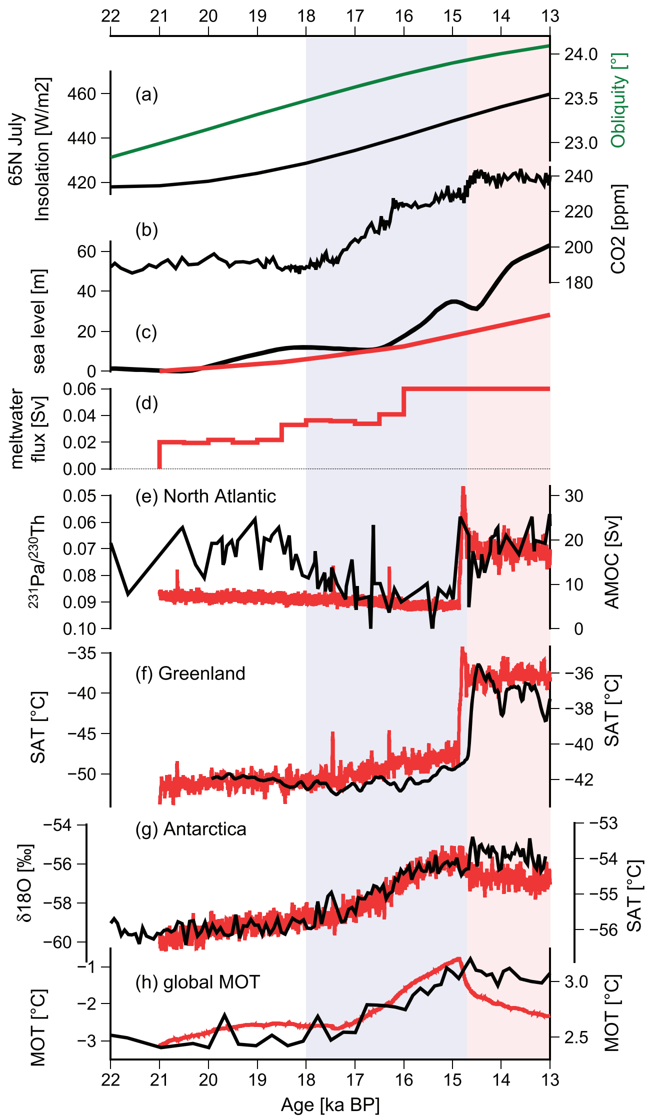

Figure 1. Model forcings and results of the REF experiment. (a) July insolation at 65°N and obliquity (Berger & Loutre, 1991); (b) atmospheric CO_2 concentration (Bereiter et al., 2015); (c) cumulative glacial meltwater in the REF experiment (red) compared with the sea level reconstruction of Lambeck et al. (2014) in black lines; (d) meltwater flux of the REF experiment. In (e–h), the model results shown in red lines are compared with reconstructions shown in black lines, and left bars indicate reconstructions, and the right bars indicate model results. (e) Streamfunction of the AMOC compared with $^{231}Pa/^{230}Th$ (Ng et al., 2018); (f) annual mean 2-m air temperature of Greenland (average of NEEM, GISP2, and NGRIP; Buizert et al., 2014); (g) annual mean 2-m air temperature of Antarctica (Dome Fuji, Kawamura et al., 2017); (h) global mean ocean temperature. The reconstructed global mean ocean temperature is relative to present day ("Mix" of Bereiter et al., 2018), and the simulated value is the raw value. The 15-year running mean is displayed for the simulated 2-m air temperature, and the vertical bars are scaled to make the amplitude of reconstructions and model results closer. The blue and red shaded areas correspond to the periods of H1 and BA, following Ivanovic, Gregoire, Kageyama, et al. (2016).

2018). However, abrupt increase in the AMOC in response to gradual forcing of the last deglaciation has not yet been shown by AOGCMs, and the respective roles of forcings in the abrupt climate changes should be clarified. Recently, a working group of the Paleoclimate Model Intercomparison Project Phase 4 (PMIP4) collected boundary conditions for climate models and proposed a protocol for transient simulation of the last deglaciation (Ivanovic, Gregoire, Kageyama, et al., 2016). In the present study, we show that from transient simulation of the last deglaciation using MIROC AOGCM mostly following the PMIP4 protocol, an abrupt recovery of the AMOC was caused by gradual boundary condition changes during the last deglaciation. We discuss the respective roles of climate forcings by analyzing the time series of simulated climate changes and by conducting sensitivity experiments.

2. Model and Experimental Design

We used MIROC 4m AOGCM, the same model as that used in a previous study (Kawamura et al., 2017). MIROC 4m is based on MIROC 3.2 (Hasumi & Emori, 2004), which contributed to the Coupled Model Intercomparison Project phase 3 and PMIP2. The resolution of the atmospheric component was T42 (about 2.8° × 2.8°) with 20 vertical levels and that of the ocean component was about 1.4° × 1° with 43 vertical levels. The MIROC 4m produced vigorous AMOC under the LGM when submitted to PMIP2 (Otto-Bliesener et al., 2007). The coefficient of the horizontal isopycnal layer thickness diffusivity of the ocean model was changed to 7.0×10^6 cm^2/s from 3.0×10^6 cm^2/s, and the present model produces weak AMOC under the LGM because of enhanced dense Antarctic Bottom Water (AABW) formation (Kawamura et al., 2017). The MIROC has been used to investigate the climate of the LGM with radiative forcing and climate feedback (Yoshimori et al., 2009), the effect of ice sheets on the climate and the AMOC (Abe-Ouchi et al., 2015; Kawamura et al., 2017; Sherriff-Tadano et al., 2018), ocean biogeochemical cycles (Kobayashi et al., 2015; Kobayashi & Oka, 2018; Yamamoto et al., 2019), and mass balance of the Antarctic ice shelves (Kusahara et al., 2015; Obase et al., 2017).

We conducted transient simulation from the LGM (21 ka) to the end of the BA transition (13 ka) by changing insolation, atmospheric greenhouse gas (GHG) concentrations, and meltwater input, following the protocol of PMIP4 (Ivanovic, Gregoire, Kageyama, et al., 2016). The model was spun-up with the condition of the LGM lasting for more than 30,000 years, and the orbital parameters and atmospheric GHG concentrations changed over time based on reconstructions (Figures 1a and 1b, Berger & Loutre, 1991; Bereiter et al., 2015; Loulergue et al., 2008; Schilt et al., 2010). The coastlines, bathymetry, and ice sheet height and extent were fixed to those of the LGM throughout the experiment to remove the complex influence of ice sheets on the AMOC. The time series of glacial meltwater flux was uniformly applied to 50–70°N in the North Atlantic following a conventional method (Kageyama et al., 2013). The time series of meltwater was from an ice sheet reconstruction (Ice-6G) following PMIP4 (Figure 1c), and the cumulative meltwater was applied not to exceed the sea level rise since the LGM. As the meltwater flux was applied uniformly to the fixed area of the North Atlantic within 50–70°N, and meltwater input into the other ocean

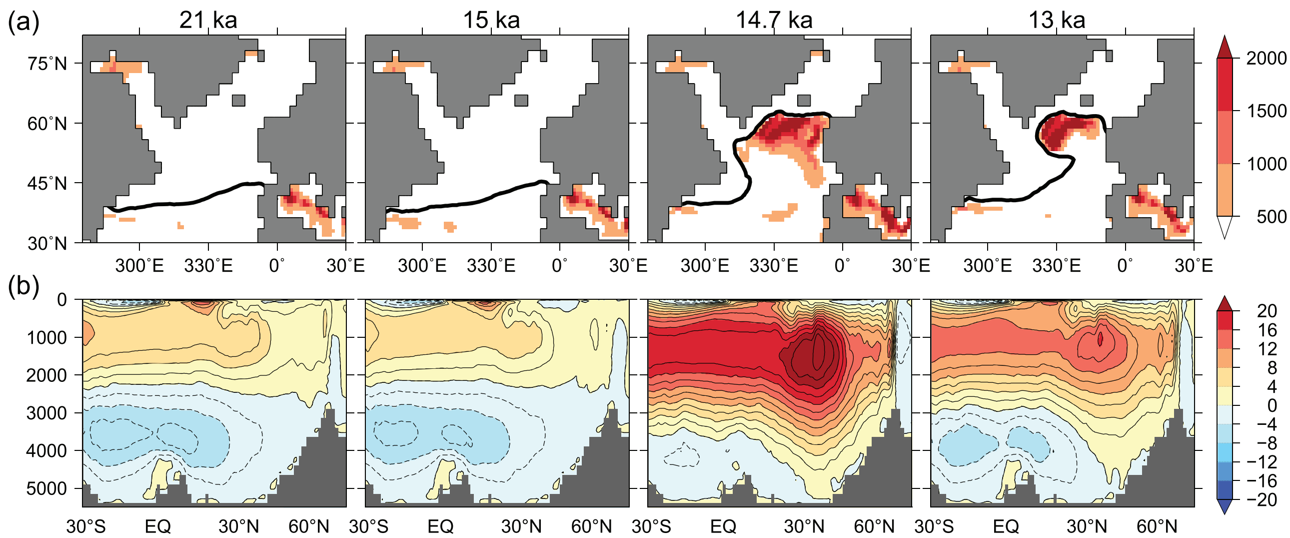

Figure 2. Results of the REF experiment: Atlantic 100-year climatologies are displayed for four different time slices. (a) The bold line indicates the sea ice edge (defined by 15% sea ice concentration), and the colors indicate the depth of the winter mixed layer [m] (defined by the density threshold of 0.125 kg/m^3). (b) Atlantic meridional ocean streamfunction [Sv].

basins was not considered, the cumulative meltwater input into the North Atlantic was less than the actual sea level rise (Figure 1d). There was no large reduction in meltwater input, as indicated by a three-dimensional dynamic ice sheet model (Abe-Ouchi et al., 2013). The amount of seawater applied to the North Atlantic was collected from the rest of the global ocean to maintain the global salinity and freshwater content, as well as bathymetry. The global salinity content was assumed to be the same as the present day. We first conducted a number of experiments that differed in the time series of meltwater fluxes and found that the timing of abrupt increase in the AMOC depended on the meltwater flux (Supporting Information, Figure S1). We selected one experiment to serve as a reference experiment (REF), as the timing of BA warming was close to reconstructions (red lines of Figure 1). In the REF experiment, the time series of the meltwater input followed the reconstructed volume of the Northern Hemisphere ice sheet (ICE-6G, Peltier et al., 2015) during 21 to 16 ka, and the meltwater flux was kept to 0.06 Sv thereafter (Figure 1d).

3. Results

In our simulations, we found that the abrupt increase in the AMOC could be caused without reduction in meltwater. In the REF experiment, a relatively weak AMOC (7 to 8 Sv) compared with the present-day simulation (16 Sv) continued from the LGM to H1 (Figure 1e). The AMOC did not weaken during H1, as the meltwater had no peak at this time in this experiment. At the beginning of the BA transition, the AMOC abruptly strengthened to about 30 Sv. The abrupt increase in AMOC strength across the BA transition was consistent with reconstructions based on kinematic proxies of Pa/Th (Figure 1e, Ng et al., 2018). The Greenland surface air temperature abruptly rose as the AMOC strengthened (Figure 1f). Although the simulated temperature changes were smaller than those of reconstructions, it is notable that the speed of the warming event was consistent with surface temperature reconstructions (Buizert et al., 2014). Antarctic warming stopped soon after the recovery of the AMOC (Figure 1g), and a cooling trend continued for ~2,000 years, as recorded in Antarctic ice cores (Kawamura et al., 2017), as the AMOC maintained a vigorous mode. The global mean ocean temperature turned into a cooling trend after the BA transition (Figure 1h), similar to the Antarctic temperature, which was consistent with reconstructions based on atmospheric noble gas concentrations (Bereiter et al., 2018).

The abrupt climate change accompanied large changes in sea ice and deep water formation in the North Atlantic. At 21 ka (LGM), the winter sea ice edge in the North Atlantic was close to ~30°N, and the deep water formation in the North Atlantic was weak (Figure 2). The winter sea ice extent at the LGM was consistent with reconstructions (de Vernal et al., 2005). The sea ice extent and the AMOC at 15 ka were similar to those of the LGM, probably because the state of the AMOC was weak throughout this period. The winter

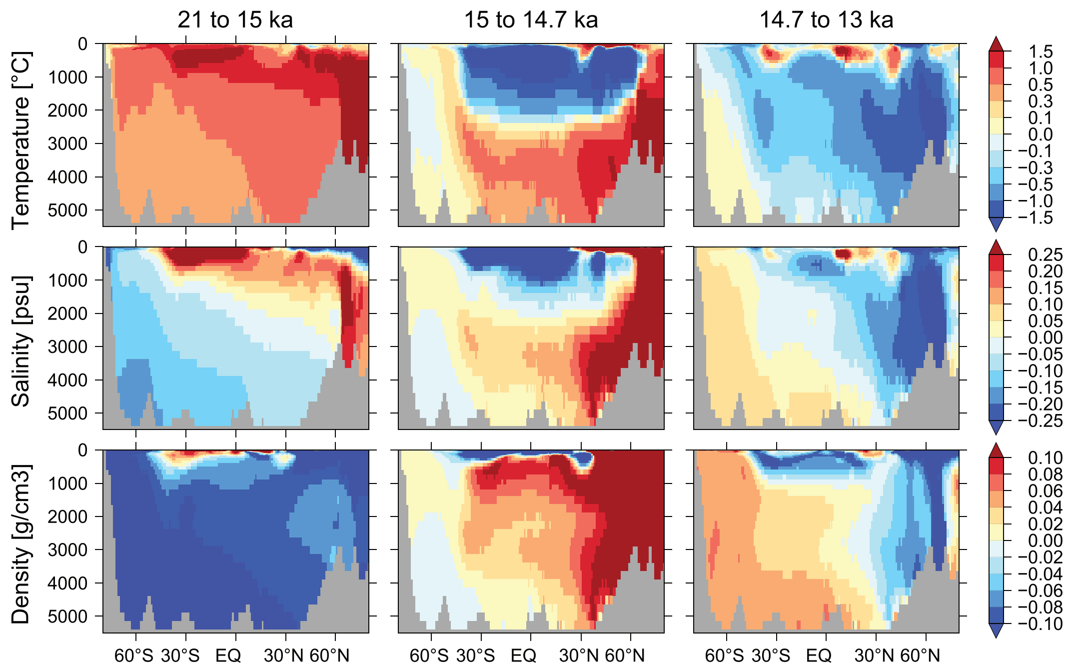

Figure 3. Results of the REF experiment: zonal mean ocean temperature, salinity, and density differences for three time slices, averaged for the Atlantic Ocean.

sea ice retreated to about 60°N at 14.7 ka, and this retreat of sea ice initiated the deep water formation and associated convective mixing (Figure 2). This change triggered a drastic release of heat stored in the subsurface of the North Atlantic by wintertime sea surface cooling and increased heat transport from the South Atlantic (Figure 3), which promoted further retreat of sea ice. The winter sea ice expanded slightly at 13 ka, and a strong AMOC persisted. These changes in the North Atlantic sea ice and ocean associated with abrupt resumption of the AMOC are consistent with previous studies (Buizert et al., 2014; Zhang et al., 2017; Zhu et al., 2014). Although there was little change in sea ice extent and meridional overturning circulation in the North Atlantic between 21 to 15 ka, there was gradual but steady change in the deep Atlantic Ocean, characterized by warming and freshening at the bottom of the Atlantic Ocean (Figure 3). This gradual change was likely induced by warming and sea ice melting in the Southern Ocean, which promoted warming and freshening of bottom water of the North Atlantic by the AABW cell (Liu et al., 2015). The gradual warming and freshening of the bottom of the North Atlantic contributed to weakened stratification in the North Atlantic (Figure S2). From 15 to 14.7 ka, the tendencies of the temperature and salinity changed significantly as a result of the overshoot in the AMOC. The salinity and density trends during 14.7 to 13 ka were similar to the reverse of 21 to 15 ka. Therefore, gradual warming of the deglaciation caused gradual weakening of the stratification of the North Atlantic and finally caused the drastic retreat of sea ice and initiation of deep convection. We calculated Mov, a stability index of the AMOC defined by freshwater transport across the Southern and Northern boundaries of the Atlantic (Liu et al., 2015). Mov was negative from the LGM to H1 and had decreasing trend, and it changed to positive as soon as the AMOC recovered at the BA transition (Figure S3). A decrease in the salinity of South Atlantic contributed to the increase in Mov (Figure S4) as Figure 4 of Liu et al. (2015). This change of Mov during the deglaciation has large similarity between our study and Liu et al. (2015), despite the relation between AMOC change and meltwater was very different.

The global map of surface air temperature changes indicates that the temperature changes differed between the stages of the deglaciation (Figure 4a). The surface temperature change exhibited warming in both polar regions, whereas the tropics exhibited slight cooling from 21 to 18 ka. This temperature change was likely induced by the increase of obliquity, as the CO_2 rise during this period was small. The surface temperature increased globally from 18 to 16 ka, as the rise of CO_2 in this period overwhelmed orbital forcing. The Antarctic region exhibited greater warming from 16 to 15 ka, before the BA transition. The period of 15 to

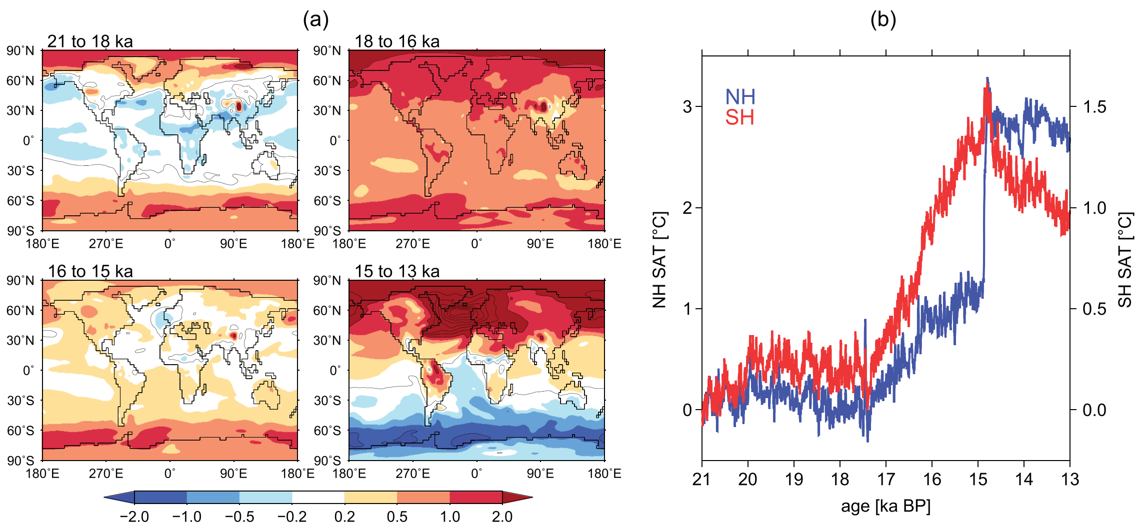

Figure 4. Results of the REF experiment: (a) surface air temperature changes from four time periods; (b) time series of temperature averaged in both hemispheres (difference from 21 ka, and different vertical scales are used).

13 ka, across the BA transition, was characterized by drastic warming in the Northern Hemisphere and gradual cooling in the Southern Hemisphere, consistent with the pattern of AMOC resumption (Pedro et al., 2018). The surface temperature averaged for the both hemispheres also showed that bipolar climate change occurred after the BA transition and that the cooling trend of the Southern Hemisphere continued for more than 1,000 years (Figure 4b).

We also found that the timing of abrupt increase in the AMOC was affected by the flux of meltwater. If no meltwater was applied (green lines of Figure 5a), an abrupt recovery in the AMOC occurred at around 19 ka. If the meltwater was less than that of the REF experiment (blue lines of Figure 5a), an abrupt recovery of the AMOC occurred at ~16 ka, earlier than in reconstructions. We compared simulated surface temperature change at NEEM, Greenland with nitrogen isotopes as an indicator of abrupt surface temperature change (Rosen et al., 2014). The simulated abrupt warming in Greenland temperature occurred within 100 years in both simulations, which were consistent with the reconstruction (Figure 5b). These results indicate that small changes in the meltwater flux may affect the timing in the abrupt increase in the AMOC but do not affect the abruptness of the increase in the AMOC and surface temperature changes in Greenland.

4. Discussion

As a summary of the results, from transient simulations of the last deglaciation, we found that an abrupt increase in the AMOC could be caused without stopping meltwater in the North Atlantic. The results of the present study are consistent with previous studies in that gradual background climate change can cause abrupt increase in the AMOC, with an ocean general circulation model (Knorr & Lohmann, 2003; Knorr & Lohmann, 2007) and Earth system model of intermediate complexity (Ganopolski & Roche, 2009), and an AOGCM under gradual change in atmospheric CO_2 (Zhang et al., 2017). The new finding and strength of the study is that abrupt BA-like climate change can be simulated by an atmosphere-ocean coupled GCM under reconstructed forcing of insolation and GHGs of the last deglaciation, and meltwater from ice sheets. As found in Antarctic Ocean temperature, salinity, and density changes before the BA transition (Figure 3), we speculate that gradual warming freshened and warmed the Southern Ocean through reduction in sea ice production and formation of AABW (Kawamura et al., 2017; Liu et al., 2005). The AABW affected the water mass of the bottom water of the North Atlantic, and the threshold of the resumption of the AMOC was exceeded by the resumption of the AMOC by overcoming the effect of meltwater, which acted to weaken the AMOC. Since a critical question is the stability of the AMOC, we analyzed a stability indicator of the AMOC. Mov in this study is very similar to the previous study of the last deglaciation (Liu et al., 2015), despite the AMOC change in the present study is caused by the gradual warming, not a reduction in meltwater. Abrupt increase in indicator of the stability seems to be a response to the changes in the AMOC,

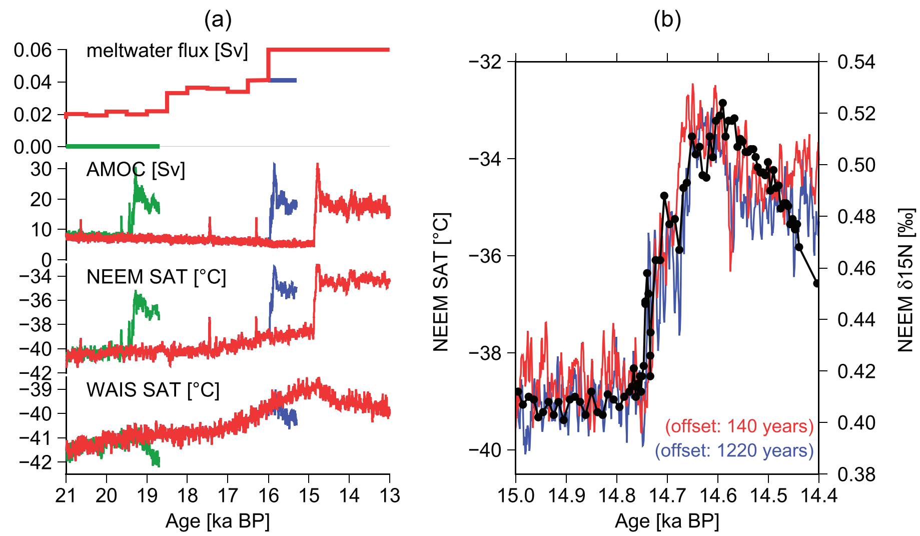

Figure 5. (a) Experimental design and results of the sensitivity experiments. Experimental design of the meltwater input, model results of AMOC streamfunction, and annual mean 2-m air temperature at NEEM (Greenland) and WAIS (Antarctica) are displayed. The red lines indicate the REF experiment (same as Figure 1), the meltwater after 16 ka was less than in the REF experiment in the experiment indicated by blue lines, and the meltwater was not applied at all in the experiment indicated by green lines. (b) The black lines indicate reconstructed Greenland surface air temperature at NEEM (Rosen et al., 2014) and simulated annual mean 2-m air temperature at NEEM in the REF experiment (red line) and one sensitivity experiment (blue lines). The model years were offset by 140 and 1,220 years, respectively, to match the timing of abrupt warming.

and therefore it may be difficult to forecast the timing of abrupt increase in the AMOC from the stability index. The relative contributions of the processes that affected the abrupt changes in the AMOC should be clarified in the future.

The sensitivity experiments demonstrated that the timing of abrupt increase in the AMOC depended on the meltwater. A notable point is that BA-like climate change occurred at 19 ka, in a very early stage of the last deglaciation, if meltwater flux was not applied at all, as shown in green lines in Figure 5a. In this experiment, the model was forced only by orbital parameters and atmospheric GHGs. The surface temperature trends in the early stage of the last deglaciation exhibited warming in the polar regions and cooling in the tropics (Figure 4a), indicating that increase in obliquity (Figure 1a) was the primary forcing of this period. Therefore, the results of the green line experiment suggest that gradual forcing of insolation, mainly by obliquity, could also induce abrupt climate changes. This result is consistent with a previous study in that under lower CO_2, high obliquity enhances the AMOC by reducing the AABW (Galbraith & de Lavergne, 2019). In the REF experiment, continuous meltwater from the LGM contributed to preventing BA-like climate changes for about several thousand years, by freshening the sea surface and strengthening the stratification of the North Atlantic.

The simulated patterns of surface temperature changes reflect different forcing and climate responses of the last deglaciation. Gradual increase in obliquity warmed the polar regions of both hemispheres in the early stage of the last deglaciation (21 to 18 ka), consistent with reconstructions (WAIS Project Members, 2013). For the period of 18 to 16 ka, the reconstruction indicates that there was significant warming in the Southern Hemisphere (Shakun et al., 2012), but the model shows warming in both hemispheres with weak warming of the Southern Hemisphere (Figure 4b). We speculate that this was because sea ice change during H1 was too small and surface temperature changes were overwhelmed by GHGs. The simulated AMOC strength during H1 was not so weak compared with the LGM (Figure 1d), which may be inconsistent with proxies. Improved representation of H1 by improving the meltwater scheme should be investigated in the future. Reconstructions from North Pacific regions suggest that synchronous warming between the North Pacific and Greenland started earlier than the BA transition (Praetorius & Mix, 2014). The pattern of surface temperature change suggests that global warming induced by GHGs may produce synchronous warming between distant areas (Figure 4a).

Several boundary conditions were simplified in the present study compared with reality. First, the area of meltwater input in the North Atlantic was constant over time. The meltwater should have reached various ocean basins outside the North Atlantic through river runoff (Clark et al., 2001; Ivanovic et al., 2016; Tarasov & Peltier, 2005). Previous studies have indicated that different regions of meltwater flux produce different responses of the AMOC (Otto-Bliesner & Brady, 2010; Roche et al., 2009; Weaver et al., 2003). Second, the ice sheet configurations in the Northern Hemisphere that affect the AMOC were kept to those of the LGM. In particular, the winds over the Atlantic Ocean, critical to the AMOC (Oka et al., 2012), would be significantly influenced by the Laurentide Ice Sheet (Sherriff-Tadano et al., 2018). As shown by Zhu et al. (2014), the gradual retreat of the Northern Hemisphere ice sheet may have weakened the AMOC and affected abrupt climate changes. The impacts of improved representation of these ice sheet boundary conditions should be clarified in the future.

Reconstruction has indicated that the warm period of the BA persisted until the Younger Dryas, for about 1,700 years. At roughly the same time as the BA transition, there was a rapid sea level rise called meltwater pulse 1A (Deschamps et al., 2012). The sea level rise of this period corresponds to meltwater flux of ~0.4 Sv, significantly higher than the applied meltwater in the present study. We did not take into account such drastic increase in meltwater flux, as the AMOC would have significantly decreased if such an amount of meltwater were applied to the North Atlantic (Bethke et al., 2012; Ivanovic et al., 2018). As the meltwater from ice sheets flows into different ocean basins by river runoff (Ivanovic, Gregoire, Wickert, et al., 2016), the relationship between meltwater pulse 1A and vigorous AMOC during BA is beyond the scope of this study.

The present study has implications for the chain of events during the glacial termination. During the early stage of the last deglaciation, rising summer insolation led to melting continental ice sheets in the Northern Hemisphere, which delivered meltwater to the North Atlantic and weakened the AMOC during the Heinrich events (Denton et al., 2010). The reduced AMOC warmed the Southern Ocean through the bipolar seesaw mechanism and raised atmospheric CO_2 (Menviel et al., 2014). As found in the present study, gradual increase in atmospheric CO_2 during H1 may have contributed to cause warming and freshening in the deep water and weakened stratification of the North Atlantic. This may have contributed to the abrupt increase in the AMOC during the BA transition, much earlier than the end of the last glacial termination. However, from comparison of the last four deglaciations, not all deglaciations accompanied BA-like climate changes as in the last deglaciation (Cheng et al., 2009). We expect further investigations on the critical processes, and model-data comparisons will improve understanding of the nature of the climate system during deglaciations in the past.

Acknowledgments
This research was supported by JSPS KAKENHI Grants 17H06104 and 17H06323. We performed numerical simulations on the Earth Simulator 3 at Japan Agency for Marine-Earth Science and Technology (JAMSTEC). We appreciate the work of the two anonymous reviewers for helpful comments and constructive suggestions. We thank Sara J. Mason, M.Sc., from Edanz Group (www.edanzediting.com/ac) for editing a draft of this manuscript. The presented model data are available from the repository of Center for Earth Surface System Dynamics, Atmosphere and Ocean Research Institute, The University of Tokyo (http://cesd.aori.u-tokyo.ac.jp/index_en.html).

References

Abe-Ouchi, A., Saito, F., Kageyama, M., Braconnot, P., Harrison, S. P., Lambeck, K., et al. (2015). Ice-sheet configuration in the CMIP5/PMIP3 Last Glacial Maximum experiments. *Geoscientific Model Development*, *8*(11), 3621–3637. https://doi.org/10.5194/gmd-8-3621-2015

Abe-Ouchi, A., Saito, F., Kawamura, K., Raymo, M. E., Okuno, J., Takahashi, K., & Blatter, H. (2013). Insolation-driven 100,000-year glacial cycles and hysteresis of ice-sheet volume. *Nature*, *500*, 190–193. https://doi.org/10.1038/nature12374

Bereiter, B., Eggleston, S., Schmitt, J., Nehrbass-Ahles, C., Stocker, T. F., Fischer, H., et al. (2015). Revision of the EPICA Dome C CO_2 record from 800 to 600 kyr before present. *Geophysical Research Letters*, *42*, 542–549. https://doi.org/10.1002/2014GL061957

Bereiter, B., Shackleton, S., Baggenstos, D., Kawamura, K., & Severinghaus, J. (2018). Mean global ocean temperatures during the last glacial termination. *Nature*, *553*, 39–44. https://doi.org/10.1038/nature25152

Berger, A., & Loutre, M. F. (1991). Insolation values for the climate of the last 10 million years. *Quaternary Sciences Review*, *10*(4), 297–317. https://doi.org/10.1016/0277-3791(91)90033-Q

Bethke, I., Li, C., & Nisancioglu, K. H. (2012). Can we use ice sheet reconstructions to constrain meltwater for deglacial simulations? *Paleoceanography*, *27*, PA2205. https://doi.org/10.1029/2011PA002258

Broecker, W. S. (1998). Paleocean circulation during the last deglaciation: A bipolar seesaw? *Paleoceanography*, *13*(2), 119–121. https://doi.org/10.1029/97PA03707

Brown, N., & Galbraith, E. D. (2016). Hosed vs. unhosed: Interruptions of the Atlantic meridional overturning circulation in a global coupled model, with and without freshwater forcing. *Climate of the Past*, *12*, 1663–1679. https://doi.org/10.5194/cp-12-1663-2016

Buizert, C., Gkinis, V., Severinghaus, J. P., He, F., Lecavalier, B. S., Kindler, P., et al. (2014). Greenland temperature response to climate forcing during the last deglaciation. *Science*, *345*(6201), 1177–1180. https://doi.org/10.1126/science.1254961

Carlson, A. E., & Clark, P. U. (2012). Ice sheet sources of sea level rise and freshwater discharge during the last deglaciation. *Reviews of Geophysics*, *50*, RG4007. https://doi.org/10.1029/2011rg000371

Cheng, H., Edwards, R. L., Broecker, W. S., Denton, G. H., Kong, X., Wang, Y., et al. (2009). Ice age terminations. *Science*, *326*(5950), 248–252. https://doi.org/10.1126/science.1177840

Clark, P. U., Marshall, S. J., Clarke, G. K. C., Hostetler, S. W., Licciardi, J. M., & Teller, J. T. (2001). Freshwater forcing of abrupt climate change during the Last Glaciation. *Science*, *293*(5528), 283–287. https://doi.org/10.1126/science.1062517.

Clark, P. U., Pisias, N. G., Stocker, T. F., & Weaver, A. J. (2002). The role of the thermohaline circulation in abrupt climate change. *Nature*, *415*(6874), 863–869. https://doi.org/10.1038/415863a

Clark, P. U., Shakun, J. D., Baker, P. A., Bartlein, P. J., Brewer, S., Brook, E., et al., et al. (2012). Global climate evolution during the last deglaciation. *Proceedings of the National Academy of Sciences*, *109*(19), E1134–E1142. https://doi.org/10.1073/pnas.1116619109

Denton, G. H., Anderson, R. F., Toggweiler, J. R., Edwards, R. L., Schaefer, J. M., & Putnam, A. E. (2010). The Last Glacial termination. *Science*, *328*, 1652–1656. https://doi.org/10.1126/science.1184119

Deschamps, P., Durand, N., Bard, E., Hamelin, B., Camoin, G., Thomas, A. L., et al. (2012). Ice-sheet collapse and sea-level rise at the Bolling warming 14,600 years ago. *Nature*, *483*, 559–564. https://doi.org/10.1038/nature10902

de Vernal, A., Eynaud, F., Henry, M., Hillaire-Marcel, C., Londeix, L., Mangin, S., et al. (2005). Reconstruction of sea-surface conditions at middle to high latitudes of the Northern Hemisphere during the Last Glacial Maximum (LGM) based on dinoflagellate cyst assemblages. *Quaternary Science Reviews*, *24*, 897–924. https://doi.org/10.1016/j.quascirev.2004.06.014

Galbraith, E., & de Lavergne, C. (2019). Response of a comprehensive climate model to a broad range of external forcings: Relevance for deep ocean ventilation and the development of late Cenozoic ice ages. *Climate Dynamics*, *52*(1-2), 653–679. https://doi.org/10.1007/s00382-018-4157-8

Ganopolski, A., & Roche, D. M. (2009). On the nature of lead-lag relationships during glacial-interglacial climate transitions. *Quaternary Science Reviews*, *28*, 3361–3378. https://doi.org/10.1016/j.quascirev.2009.09.019

Hasumi, H., & Emori, S. (2004), K-1 coupled model (MIROC) description, K-1 Tech. Rep.1, 34 pp. Center for Climate System Center Res., University of Tokyo, Tokyo.

He, F., Shakun, J. D., Clark, P. U., Carlson, A. E., Liu, Z., Otto-Bliesner, B. L., & Kutzbach, J. E. (2013). Northern Hemisphere forcing of Southern Hemisphere climate during the last deglaciation. *Nature*, *494*, 81–85. https://doi.org/10.1038/nature11822

Ivanovic, R. F., Gregoire, L. J., Kageyama, M., Roche, D. M., Valdes, P. J., Burke, A., et al. (2016). Transient climate simulations of the deglaciation 21-9 thousand years before present (version 1)—PMIP4 core experiment design and boundary conditions. *Geoscientific Model Development*, *9*, 2563–2587. https://doi.org/10.5194/gmd-9-2563-2016

Ivanovic, R. F., Gregoire, L. J., Wickert, A. D., & Burke, A. (2018). Climatic effect of Antarctic meltwater overwhelmed by concurrent Northern Hemispheric melt. *Geophysical Research Letters*, *45*, 5681–5689. https://doi.org/10.1029/2018GL077623

Ivanovic, R. F., Gregoire, L. J., Wickert, A. D., Valdes, P. J., & Burke, A. (2016). Collapse of the North American ice saddle 14,500 years ago caused widespread cooling and reduced ocean overturning circulation. *Geophysical Research Letters*, *44*, 383–392. https://doi.org/10.1002/2016GL071849

Kageyama, M., Merkel, U., Otto-Bliesner, B., Prange, M., Abe-Ouchi, A., Lohmann, G., et al. (2013). Climatic impacts of fresh water hosing under Last Glacial Maximum conditions: A multi-model study. *Climate of the Past*, *9*(2), 935–953. https://doi.org/10.5194/cp-9-935-2013

Kawamura, K., Abe-Ouchi, A., Motoyama, H., Ageta, Y., Aoki, S., Azuma, N., et al. (2017). State dependence of climatic instability over the past 720,000 years from Antarctic ice cores and climate modeling. *Science Advances*, *3*(2), e1600446. https://doi.org/10.1126/sciadv.1600446

Klockmann, M., Mikolajewicz, U., & Marotzke, J. (2018). Two AMOC states in response to decreasing greenhouse gas concentrations in the coupled climate model MPI-ESM. *Journal of Climate*, *31*(19), 7969–7984. https://doi.org/10.1175/JCLI-D-17-0859.1

Knorr, G., & Lohmann, G. (2003). Southern Ocean origin for the resumption of Atlantic thermohaline circulation during deglaciation. *Nature*, *424*(6948), 532–536. https://doi.org/10.1038/nature01855

Knorr, G., & Lohmann, G. (2007). Rapid transitions in the Atlantic thermohaline circulation triggered by global warming and meltwater during the last deglaciation. *Geochemistry, Geophysics, Geosystems*, *8*, Q12006. https://doi.org/10.1029/2007GC001604

Kobayashi, H., Abe-Ouchi, A., & Oka, A. (2015). Role of Southern Ocean stratification in glacial atmospheric CO_2 reduction evaluated by a three-dimensional ocean general circulation model. *Paleoceanography*, *30*, 1202–1216. https://doi.org/10.1002/2015PA002786

Kobayashi, H., & Oka, A. (2018). Response of atmospheric pCO_2 to glacial changes in the Southern Ocean amplified by carbonate compensation. *Paleoceanography and Paleoclimatology*, *33*, 1206–1229. https://doi.org/10.1029/2018PA003360

Kusahara, K., Sato, T., Oka, A., Obase, T., Greve, R., Abe-Ouchi, A., & Hasumi, H. (2015). Modelling the Antarctic marine cryosphere at the Last Glacial Maximum. *Annals of Glaciology*, *56*(69), 425–435. https://doi.org/10.3189/2015AoG69A792

Lambeck, K., Rouby, H., Purcell, A., Sun, Y., & Sambridge, M. (2014). Sea level and global ice volumes from the Last Glacial Maximum to the Holocene. *Proceedings of the National Academy of Sciences*, *111*(43), 15296–15303. https://doi.org/10.1073/pnas.1411762111

Liu, W., Liu, Z., Cheng, J., & Hu, H. (2015). On the stability of the Atlantic meridional overturning circulation during the last deglaciation. *Climate Dynamics*, *44*(5-6), 1257–1275. https://doi.org/10.1007/s00382-014-2153-1

Liu, Z., Otto-Bliesner, B. L., He, F., Brady, E. C., Tomas, R., Clark, P. U., et al. (2009). Transient simulation of last deglaciation with a new mechanism for Bolling-Allerod warming. *Science*, *325*(5938), 310–314. https://doi.org/10.1126/science.1171041

Liu, Z., Shin, S.-I., Webb, R. S., Lewis, W., & Otto-Bliesner, B. L. (2005). Atmospheric CO_2 forcing on glacial thermohaline circulation and climate. *Geophysical Research Letters*, *32*, L02706. https://doi.org/10.1029/2004GL021929

Loulergue, L., Schilt, A., Spahni, R., Masson-Delmotte, V., Blunier, T., Lemieux, B., et al. (2008). Orbital and millennial-scale features of atmospheric CH4 over the past 800,000 years. *Nature*, *453*(7193), 383–386. https://doi.org/10.1038/nature06950

McManus, J. F., Francois, R., Gherardi, J.-M., Keigwin, L. D., & Brown-Leger, S. (2004). Collapse and rapid resumption of Atlantic meridional circulation linked to deglacial climate changes. *Nature*, *428*(6985), 834–837. https://doi.org/10.1038/nature02494

Menviel, L., England, M. H., Meissner, K. J., Mouchet, A., & Yu, J. (2014). Atlantic-Pacific seesaw and its role in outgassing CO2 during Heinrich events. *Paleoceanography*, *29*, 1–13. https://doi.org/10.1002/2013PA002542

Menviel, L., Timmermann, A., Timm, O. E., & Mouchet, A. (2011). Deconstructing the last glacial termination: The role of millennial and orbital-scale forcings. *Quaternary Science Reviews*, *30*(9-10), 1155–1172. https://doi.org/10.1016/j.quascirev.2011.02.005

Ng, H. C., Robinson, L. F., McManus, J. F., Mohamed, K. J., Jacobel, A. W., & Ivanovic, R. F. (2018). Coherent deglacial changes in western Atlantic Ocean circulation. *Nature Communications*, *9*(1), 2947. https://doi.org/10.1038/s41467-018-05312-3

Obase, T., Abe-Ouchi, A., Kusahara, K., Hasumi, H., & Ohgaito, R. (2017). Responses of basal melting of Antarctic ice shelves to the climatic forcing of the Last Glacial Maximum and CO_2 doubling. *Journal of Climate*, *30*(10), 3473–3497. https://doi.org/10.1175/JCLI-D-15.0908.1

Oka, A., Hasumi, H., & Abe-Ouchi, A. (2012). The thermal threshold of the Atlantic meridional overturning circulation and its control by wind stress forcing during glacial climate. *Geophysical Research Letters*, *39*, L09709. https://doi.org/10.1029/2012GL051421

Otto-Bliesener, B. L., Hewitt, C. D., Marchitto, T. M., Brady, E., Abe-Ouchi, A., Crucifix, M., et al. (2007). Last Glacial Maximum ocean thermohaline circulation: PMIP2 model intercomparisons and data constraints. *Geophysical Research Letters*, *34*, L12706. https://doi.org/10.1029/2007GL029475

Otto-Bliesner, B. L., & Brady, E. C. (2010). The sensitivity of the climate response to the magnitude and location of freshwater forcing: Last Glacial Maximum experiments. *Quaternary Science Reviews*, *29*, 56–73. https://doi.org/10.1016/j.quascirev.2009.07.004

Pedro, J. B., Bostock, H. C., Bitz, C. M., He, F., Vandergoes, M. J., Steig, E. J., et al. (2016). The spatial extent and dynamics of the Antarctic cold reversal. *Nature Geoscience*, *9*, 51–56. https://doi.org/10.1038/NGEO2580

Pedro, J. B., Jochum, M., Buizert, C., He, F., Barker, S., & Rasmussen, S. O. (2018). Beyond the bipolar seesaw: Toward a process understanding of interhemispheric coupling. *Quaternary Science Reviews*, *192*, 27–46. https://doi.org/10.1016/j.quascirev.2018.05.005

Peltier, W. R., Argus, D. F., & Drummond, R. (2015). Space geodesy constrains ice age terminal deglaciation: The global ICE-6G_C (VM5a) model. *Journal of Geophysical Research: Solid Earth*, *120*, 450–487. https://doi.org/10.1002/2014JB011176

Praetorius, S. K., & Mix, A. C. (2014). Synchronization of North Pacific and Greenland climates preceded abrupt deglacial warming. *Science*, *345*(6195), 444–448. https://doi.org/10.1126/science.1252000

Rahmstorf, S. (2002). Ocean circulation and climate during the past 120,000 years. *Nature*, *419*, 207–214. https://doi.org/10.1038/nature01090

Roberts, N. L., Piotrowski, A. M., McManus, J. F., & Keigwin, L. D. (2010). Synchronous deglacial overturning and water mass source changes. *Science*, *327*(5961), 75–78. https://doi.org/10.1126/science.1178068

Roche, D. M., Wiersma, A. P., & Renssen, H. (2009). A systematic study of the impact of freshwater pulses with respect to different geographical locations. *Climate Dynamics*, *34*(7-8), 997–1013. https://doi.org/10.1007/s00382-009-0578-8

Rosen, J. L., Brook, E. J., Severinghaus, J. P., Blunier, T., Mitchell, L. E., Lee, J. E., et al. (2014). An ice core record of near-synchronous global climate changes at the Bolling transition. *Nature Geoscience*, *7*, 459–463. https://doi.org/10.1038/NGEO2147

Schilt, A., Baumgartner, M., Schwander, J., Buiron, D., Capron, E., Chappellaz, J., et al. (2010). Atmospheric nitrous oxide during the last 140 000 years. *Earth and Planetary Science Letters*, *300*(1-2), 33–43. https://doi.org/10.1016/j.epsl.2010.09.027

Shakun, J. D., & Carlson, A. E. (2010). A global perspective on Last Glacial Maximum to Holocene climate change. *Quaternary Science Reviews*, *29*, 1801–1816. https://doi.org/10.1016/j.quascirev.2010.03.016

Shakun, J. D., Clark, P. U., He, F., Marcott, S. A., Mix, A. C., Liu, Z., et al. (2012). Global warming preceded by increasing carbon dioxide concentrations during the last deglaciation. *Nature*, *484*, 49–54. https://doi.org/10.1038/nature10915

Sherriff-Tadano, S., Abe-Ouchi, A., Yoshimori, M., Oka, A., & Chan, W. (2018). Influence of glacial ice sheets on the Atlantic meridional overturning circulation through surface wind change. *Climate Dynamics*, 1–23. https://doi.org/10.1007/s00382-017-3780-0

Tarasov, L., & Peltier, W. R. (2005). Arctic freshwater forcing of the Younger Dryas cold reversal. *Nature*, *435*, 662–665. https://doi.org/10.1038/nature03617

WAIS Divide Project Members (2013). Onset of deglacial warming in West Antarctica driven by local orbital forcing. *Nature*, *500*, 440–444. https://doi.org/10.1038/nature12376

Weaver, A. J., Saenko, O. A., Clark, P. U., & Mitrovica, J. X. (2003). Meltwater Pulse 1A from Antarctica as a trigger of the Bolling-Allerod warm interval. *Science*, *299*(5613), 1709–1713. https://doi.org/10.1126/science.1081002

Yamamoto, A., Abe-Ouchi, A., Ohgaito, R., Ito, A., & Oka, A. (2019). Glacial CO_2 decrease and deep-water deoxygenation by iron fertilization from glaciogenic dust. *Climate of the Past*, *15*, 981–996. https://doi.org/10.5194/cp-15-981-2019

Yoshimori, M., Yokohata, T., & Abe-Ouchi, A. (2009). A comparison of climate feedback strength between CO_2 doubling and LGM experiments. *Journal of Climate*, *22*, 3374–3395. https://doi.org/10.1175/2009JCLI2801.1

Zhang, X., Knorr, G., Lohmann, G., & Barker, S. (2017). Abrupt North Atlantic circulation changes in response to gradual CO_2 forcing in a glacial climate state. *Nature Geoscience*, *10*(7), 518–523. https://doi.org/10.1038/NGEO2974

Zhu, J., Liu, Z., Zhang, X., Eisenman, I., & Liu, W. (2014). Linear weakening of the AMOC in response to receding glacial ice sheets in CCSM3. *Geophysical Research Letters*, *41*, 6252–6258. https://doi.org/10.1002/2014GL060891